

Accepted Manuscript

Title: Establishing whether the structural feature controlling the mechanical properties of starch films is molecular or crystalline

Author: Ming Li Fengwei Xie Jovin Hasjim Torsten Witt
Peter J. Halley Robert G. Gilbert



PII: S0144-8617(14)00933-3
DOI: <http://dx.doi.org/doi:10.1016/j.carbpol.2014.09.036>
Reference: CARP 9293

To appear in:

Received date: 23-4-2014
Revised date: 5-7-2014
Accepted date: 2-9-2014

Please cite this article as: Li, M., Xie, F., Hasjim, J., Witt, T., Halley, P. J., and Gilbert, R. G., Establishing whether the structural feature controlling the mechanical properties of starch films is molecular or crystalline, *Carbohydrate Polymers* (2014), <http://dx.doi.org/10.1016/j.carbpol.2014.09.036>

This is a PDF file of an unedited manuscript that has been accepted for publication. As a service to our customers we are providing this early version of the manuscript. The manuscript will undergo copyediting, typesetting, and review of the resulting proof before it is published in its final form. Please note that during the production process errors may be discovered which could affect the content, and all legal disclaimers that apply to the journal pertain.

17

18 **Abstract**

19 The effects of molecular and crystalline structures on the tensile mechanical properties of
20 thermoplastic starch (TPS) films from waxy, normal, and high-amylose maize were
21 investigated. Starch structural variations were obtained through extrusion and hydrothermal
22 treatment (HTT). The molecular and crystalline structures were characterized using size-
23 exclusion chromatography and X-ray diffractometry, respectively. TPS from high-amylose
24 maize showed higher elongation at break and tensile strength than those from normal maize
25 and waxy maize starches when processed with 40% plasticizer. Within the same amylose
26 content, the mechanical properties were not affected by amylopectin molecular size or the
27 crystallinity of TPS prior to HTT. This lack of correlation between the molecular size,
28 crystallinity and mechanical properties may be due to the dominant effect of the plasticizer on
29 the mechanical properties. Further crystallization of normal maize TPS by HTT increased the
30 tensile strength and Young's modulus, while decreasing the elongation at break. The results
31 suggest that the crystallinity from the remaining ungelatinized starch granules has less
32 significant effect on the mechanical properties than that resulting from starch
33 recrystallization, possibly due to a stronger network from leached-out amylose surrounding
34 the remaining starch granules.

35 **Abbreviations**

36 **ANOVA**, analysis of variance; **CF**, cryo-fractured; **CM**, compression molding; **DSC**,
37 differential scanning calorimetry; **HAMS**, high-amylose maize starch; **HTT**, hydrothermal
38 treatment; **NF**, non-fractured; **NMS**, normal maize starch; **RH**, relative humidity; **SEC**, size-

39 exclusion chromatography; **SME**, specific mechanical energy; **TPS**, thermoplastic starch;
40 **WMS**, waxy maize starch; **XRD**, X-ray diffraction

41 **Key words**

42 starch, molecular structure, crystallinity, mechanical properties, hydrothermal treatment

43

Accepted Manuscript

43

44 **1. Introduction**

45 Replacing non-biodegradable conventional synthetic plastics with renewable,
46 biodegradable alternatives has become more and more desirable, as petroleum-based plastics
47 are non-renewable and degrade slowly in the environment. One potential replacement is the
48 class of thermoplastic starch (TPS) materials. Some successful TPS products are already
49 available in the market; however, their applications are limited because of the poor
50 mechanical properties and moisture resistance. To improve the properties of TPS, it is
51 important to understand better the influences on properties of starch structural changes
52 brought about by processing.

53 Native starch granules are composed of mainly two glucose macromolecules, amylose and
54 amylopectin. Amylose is mostly linear with long branches and has a molecular weight of ~
55 10^5 – 10^6 ; it is present either in amorphous or in a single helical conformation in native starch
56 granules (Jane, Xu, Radosavljevic & Seib, 1992; Lopez-Rubio, Flanagan, Gilbert & Gidley,
57 2008). Amylopectin is highly branched and has a molecular weight of ~ 10^7 – 10^9 . The
58 branches of amylopectin are arranged into clusters of double helices that aggregate into
59 crystallites in native starch granules, while the branching points are located in amorphous
60 regions; together they form the crystalline-amorphous lamellae (Pérez & Bertoft, 2010;
61 Vamadevan, Bertoft & Seetharaman, 2013; Zhu, Bertoft & Seetharaman, 2013) and
62 subsequently the growth rings.

63 Improving the mechanical properties of TPS, such as increasing tensile strength and
64 Young's modulus or decreasing the elongation at break, has been achieved by increasing
65 starch crystallinity with aging (Shogren & Jasberg, 1994; van Soest, Hulleman, de Wit &

66 Vliegenthart, 1996). In addition, TPS materials produced from high-amylose starch have
67 good mechanical properties (Li et al., 2011; Lourdin, Valle & Colonna, 1995). By producing
68 starch materials from acid-hydrolyzed starch, van Soest et al. (van Soest, Benes, de Wit &
69 Vliegenthart, 1996) found that the tensile strength of TPS was not affected by molecular
70 weight, but the elongation at break and tearing energy were higher for starch materials with
71 higher molecular weight. However, it is difficult to separate the effects of molecular weight
72 on the mechanical properties of TPS films from those of the amylose content (Walenta, Fink,
73 Weigel & Ganster, 2001) and of starch retrogradation (van Soest, Benes & De Wit, 1995).
74 Inconsistent conclusions can be found on the relationship between starch molecular weight
75 and the mechanical properties of TPS from different studies in the literature (Lloyd & Kirst,
76 1963; van Soest, Benes, de Wit & Vliegenthart, 1996; Walenta, Fink, Weigel & Ganster,
77 2001), partly due to different testing conditions and techniques, such as aging time before
78 mechanical testing.

79 In the present study, the molecular and crystalline structural changes induced by
80 processing are correlated to the mechanical properties in order to obtain a more precise
81 correlation, as distinct from previous studies (van Soest, Benes & De Wit, 1995; van Soest,
82 Benes, de Wit & Vliegenthart, 1996) correlating the acid-hydrolyzed starch structures, which
83 may be further degraded by processing, with mechanical properties. Extrusion brings multi-
84 level starch structural changes, including degradation of large amylopectin molecules and
85 disruption of crystalline and granular structures (Li, Hasjim, Xie, Halley & Gilbert, 2013;
86 Liu, Halley & Gilbert, 2010), and a higher degree of crystallinity is brought by
87 retrogradation. Previous studies often involve changing of molecular structure by acid (van
88 Soest, Benes, de Wit & Vliegenthart, 1996) or enzyme hydrolysis (Walenta, Fink, Weigel &
89 Ganster, 2001) prior to starch processing. However, these hydrolysis procedures bring
90 significant molecular degradation: acid can hydrolyze both amylose and amylopectin in the

91 amorphous regions and enzyme randomly acts along starch chains. Such changes may be
92 different from the molecular degradation induced by extrusion.

93 In this study, waxy, normal, and high-amylose maize starches (WMS, NMS, and HAMS,
94 respectively) were used as samples providing a variation in the amylose content. Starch
95 extrudates prepared in a previous study (Li, Hasjim, Xie, Halley & Gilbert, 2013) with
96 variations in the molecular and crystalline structures, while maintaining the same amylose
97 content, were used. The crystalline structure was further altered by hydrothermal treatment
98 (HTT). Size-exclusion chromatograph (SEC), X-ray diffractometry (XRD), and scanning
99 electron microscope (SEM) were used to investigate the changes in starch molecular,
100 crystalline, and film surface structures, respectively, after compression molding, aging and
101 HTT.

102 **2. Materials and Methods**

103 *2.1. Materials*

104 WMS and HAMS (Gelose 80) were obtained from National Starch Pty. Ltd. (now
105 Ingredion, Lane Cove, NSW, Australia), and NMS was supplied by New Zealand Starch Ltd.
106 (Auckland, New Zealand). The amylose contents of WMS, NMS, and HAMS starches are 0,
107 28 and 63%, respectively, as measured in a previous study (Vilaplana, Hasjim & Gilbert,
108 2012). Starch extrudates used were those prepared in a previous study (Li, Hasjim, Xie,
109 Halley & Gilbert, 2013), where glycerol and water with a ratio of 2:3 were used as
110 plasticizer, and the extrudate strands were cut using S. F. Scheer pelletizer (Model SGS25 E4,
111 Reduction Engineering, Inc., Kent, OH, USA). The extrusion processing conditions
112 (temperature, screw speed, and plasticizer content) and the average hydrodynamic radius \bar{R}_h
113 (analyzed in the previous study (Li, Hasjim, Xie, Halley & Gilbert, 2013)) are shown in

114 Table 1. The post-extrusion treatments and characterization techniques applied to the starch
115 extrudates are summarized in Table 2.

116 **2.2. Compression molding**

117 WMS, NMS, and HAMS pellets were compression-molded into starch films using a lab
118 compression molding (CM) machine. CM was carried out at 100 °C for WMS and NMS and
119 at 130 °C for HAMS, with a pressure of 7.5 MPa for 5 min, as WMS, NMS can be
120 compression-molded into homogeneous films at 100 °C, while HAMS can only form films at
121 130 °C. The resulting films were quench-cooled using a water cooling system to 35 °C before
122 they were removed. Polytetrafluoroethylene films (Dotmar EPP Pty. Ltd., Acacia Ridge,
123 QLD, Australia) were used during CM as release agents.

124 **2.3. Water sorption**

125 Representative films of WMS and HAMS were dried in a BenchTop 2K freeze dryer
126 (VirTis, Gardiner, NY, USA) overnight, and then kept in humidity chambers at 33, 54, and
127 75% relative humidity (RH, which were achieved using MgCl₂, Mg(NO₃)₂, and NaCl
128 solutions, respectively (Ferreira, Grossmann, Mali, Yamashita & Cardoso, 2009)), for 2, 4,
129 17.5, 21, and 112.5 hours. The moisture content, M_t , at time t , as the result of moisture
130 absorption, was calculated as follows:

$$131 \quad M_t (\%) = \frac{w_t - w_o}{w_o} \times 100\% \quad [1]$$

132 Here w_o and w_t are the weight after freeze drying prior to storage and that after storing in
133 humidity chambers for time t , respectively.

134 **2.4. Hydrothermal treatment**

135 NMS films and tensile dumbbell specimens were placed on petri dishes covered with
136 cellulose filter papers, and then kept in an oven at 105 °C for three days (the RH in the oven
137 was assumed to be 100%). Beakers with water were also placed in the oven to supply the
138 moisture for HTT. After the HTT, the materials were slowly cooled in the oven for an
139 additional 2 hours with the presence of moisture to prevent breakage due to the rapid drying
140 of the films at ambient humidity, which would result in brittleness. The moisture contents of
141 starch films before and after HTT were determined from weight difference after being dried
142 in the oven at 105 °C overnight.

143 **2.5. Size-exclusion chromatography**

144 WMS and HAMS extrudates and their CM films were molecularly dissolved in dimethyl
145 sulfoxide (DMSO; GR for analysis ACS, Merck & Co, Inc., Kilsyth, VIC, Australia)
146 containing 0.5% wt LiBr (ReagentPlus, Sigma–Aldrich Pty. Ltd., Castle Hill, NSW,
147 Australia) (DMSO/LiBr solution) to yield a final concentration of 1 mg/mL, and analyzed in
148 duplicates using an SEC system (Agilent 1100 series, Agilent Technologies, Waldbronn,
149 Germany) equipped with a refractive index detector (RID-10A, Shimadzu, Kyoto, Japan),
150 following the method described elsewhere (Li, Hasjim, Xie, Halley & Gilbert, 2013). Since
151 SEC separates molecules based on size (hydrodynamic volume, V_h , or the corresponding
152 hydrodynamic radius, R_h), the results are presented as SEC distributions of starch molecules,
153 denoted by $w(\log V_h)$ (Cave, Seabrook, Gidley & Gilbert, 2009).

154 **2.6. X-ray diffractometry**

155 Representative WMS, NMS and HAMS films were stored in humidity chambers at 54%
156 RH for different days at room temperature (23 °C) before the XRD measurements, while the

157 NMS films with and without HTT were stored in the same humidity chamber for 14 days.
158 While their RHs are not considered here, one expects the trend will be the same: high amylose
159 starch will retrograde more rapidly and the starch may reach to a higher degree of
160 crystallinity; however, as showed in (Shogren & Jasberg, 1994), normal maize starch showed
161 much larger sub- T_g endotherms than high-amylose cornstarch when stored at higher RH,
162 which might be due to the B-type crystallinity formed during the long-term storage among
163 the shorter branches of WMS or NMS. The crystalline structure of stored starch films was
164 analyzed using a D8 Advance X-ray diffractometer (Bruker, Madison, WI, USA), where
165 diffractograms were recorded over an angular range (2θ) of 3–40°, with a step size of 0.02°,
166 and a rate of 0.5 s per step. The radiation parameters were set at 40 kV and 30 mA. The
167 degree of crystallinity was calculated following the method of a previous study (Li, Hasjim,
168 Xie, Halley & Gilbert, 2013) using PeakFit software (Version 4.12 Sytstat Software, Inc., San
169 Jose, CA, USA):

$$\text{Crystallinity (\%)} = \frac{\sum_{i=1}^n A_{ci}}{A_t} \times 100\% \quad [2]$$

171 where A_{ci} is the area under each crystalline peak with index i , and A_t is the total area
172 (amorphous background and crystalline peaks) under the diffractogram. Each sample was
173 only analyzed once; the standard deviation (SD) of XRD results is within 1-3% as reported in
174 a previous study (Lopez-Rubio, Flanagan, Gilbert & Gidley, 2008).

175 **2.7. Scanning electron microscopy**

176 Starch pellets (before CM) and starch films (after CM) were manually fractured after
177 being frozen in liquid nitrogen. The fragments of each sample were placed onto a specimen
178 stub with double-sided carbon tape, and then coated with a thin layer of gold using a sputter

179 coater (SPI-MODULE™, SPI Supplies, West Chester, PA, USA). The surface and inner
180 structures of starch pellet and film samples were examined using a scanning electron
181 microscope (SEM, Philips XL30, Eindhoven, Netherlands) with an accelerating voltage of 3
182 kV and a spot size of 6 nm.

183 **2.8. Tensile mechanical analysis**

184 Dumbbell specimens were cut from starch films (including those after HTT) according to
185 ASTM D638-03 standards (Australian Standard AS 1683:11); the specimens were 12 mm in
186 length and 2 mm in width, and the thickness of each specimen was measured prior to tensile
187 tests. The dumbbell specimens were then conditioned for 14 days at 33, 54, and 75% RH.
188 Each dumbbell specimen was loaded on an Instron® 5543 universal testing machine (Instron
189 Pty. Ltd., Melbourne, VIC, Australia) with a constant strain rate of 5 mm·min⁻¹. Tensile
190 strength, Young's modulus, and elongation at break were determined using BlueHill software
191 (Instron Ltd., Norwood, OH, USA), following the method of van Soest et al. (van Soest,
192 Benes, de Wit & Vliegenthart, 1996). Tensile results of each sample were averaged from at
193 least five measurements.

194 **2.9. Statistical analysis**

195 Pearson's correlation analysis was performed using Minitab 16 (Minitab Inc., State
196 College, PA, USA) to analyze any correlations between starch structural features (such as
197 amylose content, \bar{R}_h , and degree of crystallinity) and the tensile mechanical properties of the
198 resulting films with a confidence level of 95.0%. A t-test with a confidence level at 95.0%
199 was also applied to compare the water absorption profiles among different starch films stored
200 at different RH. ANOVA with Tukey's pairwise comparison was applied to compare the
201 tensile mechanical properties of different starch films.

202 **3. Results**

203 **3.1. Starch structure**

204 *3.1.1. Effect of compression molding on the starch structure*

205 Starch extrudates from various extrusion conditions (Table 1) were obtained from a
206 previous study (Li, Hasjim, Xie, Halley & Gilbert, 2013) with different degrees of
207 degradation on the molecular, crystalline and granular structures due to thermal energy
208 (gelatinization) and mechanical energy (starch damage). In order to measure the tensile
209 mechanical properties, starch extrudates were compression-molded. In spite of the structural
210 changes from extrusion, the high hydraulic pressure and heat involved in CM may cause
211 further degradation on the starch molecular, crystalline and granular structures. Thus, the
212 compression temperature and time needed to be kept as low and short, respectively, as
213 possible to reduce undesirable structural changes, which can affect the properties of the films.
214 In this study, such CM condition were chosen because WMS and NMS can only form into
215 homogeneous films at ≥ 100 °C, while HAMS can only form into films at ≥ 130 °C with the
216 pressure and time conditions used here.

217 Molecular structure and granular morphology were analyzed by SEC and SEM,
218 respectively, to investigate if there were any changes in these structures after CM. There were
219 no differences in the SEC distributions of starch molecules before and after CM (Supporting
220 Information Figure S1), indicating the compression conditions chosen have not induced
221 further molecular degradation. SEM images of the non-fractured (NF) and cryo-fractured
222 (CF) surfaces (the latter is the internal structure) of WMS and HAMS films are shown in
223 Figure 2. Before CM, the HAMS extrudates displayed more roughness on the NF surface
224 than the WMS extrudates, and also showed greater discontinuity in the internal structure. The

225 greater amount of granular starch in the HAMS extrudates is due to its higher gelatinization
226 temperature (Chen, Yu, Chen & Li, 2006; Liu, Yu, Xie & Chen, 2006). After CM, both starch
227 films display a smoother surface and internal structure, indicating that the high pressure from
228 CM can compress or disrupt the granular structure (Tabi & Kovacs, 2007) and produce
229 continuous films.

230 *3.1.2. Effect of aging, relative humidity and time on starch structures*

231 Starch materials can absorb or desorb water at different RH. Changes in the amount of
232 water, which acts as plasticizer, can influence the mechanical properties of starch films. As
233 amylose and amylopectin are the main components of starch, lyophilized representative
234 WMS and HAMS films (WMS-7 and HAMS-7, for which the extrusion processing
235 conditions prior to CM are listed in Table 1) were used as models to investigate their water
236 absorption profiles when stored at 33, 54, and 75% RH (Figure 3). The starch films stored at
237 54 and 75% RH absorbed moisture quickly and the moisture content reached a plateau within
238 the first 24 h, similar to the results reported by Thunwall et al. (Thunwall, Boldizar &
239 Rigdahl, 2006). On the other hand, the moisture content of the starch films stored at 33% RH
240 slightly decreased with the storage time, possibly due to water (plasticizer) remaining in the
241 starch films lost during the storage at low RH. There were no significant differences in the
242 water absorption profiles between WMS and HAMS films when stored at 33, 54, and 75%
243 RH.

244 Representative WMS, NMS and HAMS films (WMS-7, NMS-7, and HAMS-7,
245 respectively), were aged for different days to investigate the changes in the crystalline
246 structure of starch films during conditioning time. After CM, the WMS film was amorphous
247 and the diffractogram did not show any visible change over 7 days' storage (Figure 4A);
248 however, HAMS (Figure 4C) retrograded rapidly within 1 day, but no obvious changes in the

249 diffractogram were observed thereafter. WMS and NMS produced less crystallinity than
250 HAMS due to the speed of amylose retrogradation, and the retrogradation of amylopectin
251 only changing the degree of crystallinity after long-term storage, which is similar to the
252 results of van Soest et al. (van Soest, Hullemann, de Wit & Vliegenthart, 1996). The NMS film
253 showed a weak diffraction pattern of A-type crystallinity (at 15, 17, 18, and 23°), probably
254 from the remaining ungelatinized granules (Li, Hasjim, Xie, Halley & Gilbert, 2013), after
255 CM (0 day storage) with a small amount of the V-type crystalline structure (Figure 4B). The
256 diffraction pattern of the A-type crystallinity became more apparent after 1 day storage,
257 possibly due to the realignment of the remaining crystallites during storage. The
258 diffractograms did not show any apparent changes during storage from 8 to 14 days, with the
259 degree of crystallinity being ~ 6%. Thus, the subsequent mechanical testing experiments were
260 performed on starch films after being aged for 14 days to ensure structural equilibration.

261 *3.1.3. Effect of hydrothermal treatment on starch crystalline structure*

262 The degree of crystallinity of WMS and HAMS films, observed from the XRD
263 diffractograms, did not show increases after HTT (Supporting Information Figure S1). This
264 might be because the crystalline structure formed during HTT is from the leached long-chain
265 amylose (which can form a more perfect network in a high moisture and temperature
266 environment), whereas there is no amylose in WMS, and the amount of amylose that can
267 leach out is negligible for HAMS at the HTT temperature (105°C). On the contrary, more
268 amylose may leach out from a larger number of gelatinized NMS granules (compared to
269 HAMS), explaining why it exhibited increased degree of crystallinity after HTT (Figure 5
270 and Table 3). Hence tensile mechanical testing of hydrothermal treated starch films was only
271 applied to NMS starch films. Due to sample brittleness, only NMS-1, -2, -3, and -4 were

272 suitable for mechanical testing after HTT, and their degrees of crystallinity were analyzed
273 using XRD (Table 3).

274 The crystalline patterns of the untreated starch films were the A- and V-types, whereas the
275 C- and V-types were observed after HTT, indicated by the appearance of a small peak at 5.5°
276 (Figure 5). The differences in behaviour of NMS 1 and 3 after HTT when compared to NMS
277 2 and 4 are not explored fully in this paper. The most likely reason for the observed effect is
278 that an increase in temperature gives greater mobility for chains which do not take part in the
279 remaining crystalline structures; these chains may be able to be more affected by the HTT.
280 Previous work (Li, Hasjim, Xie, Halley & Gilbert, 2013) has noted that decreases in
281 crystallinity occurred with increases in SME; however, the conditions which caused this, low
282 plasticizer and low temperature, do not seem likely to affect the ability of the starch to
283 recrystallize after HTT. The diffraction peaks of the HTT starch films were sharper and more
284 defined, indicating that the crystalline structure became more ordered. DSC results of NMS-1
285 and -3 (Supporting information Table S1) showed increases in the melting temperatures of
286 starch crystallites, confirming that the crystalline structure became more stable after HTT.

287 **3.2. Tensile mechanical properties**

288 *3.2.1. Effect of relative humidity during aging on starch film tensile properties*

289 The tensile properties of WMS and HAMS films stored at different RH are shown in Table
290 4. Films stored at a lower RH were generally more rigid, displaying higher tensile strength,
291 and Young's modulus, but lower elongation at break than those stored at a higher RH,
292 consistent with those reported by other researchers (Mali, Sakanaka, Yamashita &
293 Grossmann, 2005; Mathew & Dufresne, 2002; Shogren & Jasberg, 1994). This is ascribed to
294 the higher moisture content of film stored at higher RH (Figure 3), which can function as
295 plasticizer.

296 *3.2.2. Effect of plasticizer content and amylose content on film tensile properties*

297 Plasticizer content (glycerol and water in this case) has a similar effect on the tensile
298 mechanical properties to that of RH (Table 1). For starch films with the same amylose
299 content, significant changes in the mechanical properties only occurred when the amount of
300 plasticizer was different. Brittle starch films resulted from a lower plasticizer content
301 displayed higher tensile strength and Young's modulus, but lower elongation at break, than
302 films with the higher plasticizer content.

303 When the mechanical properties were compared among different types of starch films with
304 the same plasticizer content (Table 1 and Supporting information Table S2), HAMS films
305 exhibited higher tensile strength than WMS and NMS films, similar to results reported by
306 others (Li et al., 2011; Lourdin, Valle & Colonna, 1995). At 30% plasticizer content, WMS
307 film showed a higher tensile strength and Young's modulus than NMS film. However, at
308 40% plasticizer content, the Young's modulus and tensile strength of WMS films were not
309 significantly different from those of NMS films. Furthermore, the WMS films had similar
310 Young's modulus to the HAMS films at both plasticizer contents. At 40% plasticizer content,
311 HAMS and NMS films had higher values of elongation at break than WMS films; however,
312 at 30% plasticizer content, NMS films had higher values of elongation at break than WMS
313 and HAMS films.

314 *3.2.3. Effect of hydrothermal treatment on starch film tensile properties*

315 The tensile mechanical properties, degree of crystallinity and moisture content for the
316 NMS starch films after HTT are shown in Table 3. Starch films after HTT showed higher
317 tensile strength and Young's modulus. There were no significant differences in the moisture
318 contents, and thus the changes in the mechanical properties were probably largely related to

319 the increase in the perfectness of the crystalline structure, which reduced the ability of starch
320 chains to deform during the tensile tests.

321 ***3.3. Correlations between starch structure and tensile mechanical properties***

322 The influence of the structural features of starches on the tensile mechanical properties
323 was explored separately for WMS and HAMS films at different plasticizer contents (Table 5)
324 (as there were only two NMS films with the same plasticizer content, the correlation analysis
325 was not performed on the NMS films). The only significant correlation observed was in the
326 HAMS films with 30% plasticizer content, showing a negative correlation between \bar{R}_h and
327 tensile strength.

328 The correlations between amylose content and mechanical properties were also explored
329 among the films with the same plasticizer content. For starch films at 40% plasticizer content,
330 there was a negative correlation between elongation at break and \bar{R}_h as well as a positive
331 correlation between elongation at break and amylose content. However, such correlations
332 were not observed from the starch films with 30% plasticizer content.

333 Finally, the crystallinity changes induced by HTT were correlated with the various
334 mechanical properties. The increase in the degree of crystallinity of starch films induced by
335 HTT was accompanied by an increase in Young's modulus, although the crystallinity prior to
336 HTT did not show any significant correlations with the tensile mechanical properties (Table
337 5).

338 4. Discussion

339 Plasticizer content, amylose content and structural factors all affect the mechanical
340 properties of TPS materials. As is shown in the results, starch with higher amylose content
341 (HAMS) showed a higher tensile strength than NMS and WMS when processed with 30%
342 plasticizer. In addition, an increase in the plasticizer content resulted in a decrease in the
343 tensile strength and Young's modulus and an increase in the elongation at break. Those
344 results are similar to those reported the previous studies (Li et al., 2011; Mali, Sakanaka,
345 Yamashita & Grossmann, 2005). As the main purpose of this study is to understand the roles
346 of molecular and crystalline structures on the tensile mechanical properties of starch films,
347 the correlations among the starch structural features and the mechanical properties are
348 discussed in greater detail.

349 For the three types of starches, WMS displays the greatest variations in molecular size
350 (Table 1) among its extrudates, as the main component (amylopectin) is severely degraded
351 during extrusion (Li, Hasjim, Xie, Halley & Gilbert, 2013; Liu, Halley & Gilbert, 2010), and
352 thus it is a good model to understand the relationship between the degraded molecular
353 structure and the tensile mechanical properties. However, there were no significant
354 correlations between \bar{R}_h and the tensile mechanical properties of WMS films (Table 5).
355 Different from acid and enzyme hydrolysis, the mechanical shear only cleaved a small
356 number of glycosidic bonds in amylopectin molecules, as explained previously (Li, Hasjim,
357 Xie, Halley & Gilbert, 2013), and the degraded amylopectin was still relatively large with a
358 vast number of short branches. During extrusion and storage, the shorter branches of
359 amylopectin may form intramolecular interactions; however, these interactions may not be
360 varied sufficiently by the extrusion processing to cause significant changes in the tensile
361 mechanical properties of WMS film. On the other hand, a negative correlation between \bar{R}_h

362 and tensile strength was observed with HAMS films at 30% plasticizer content (Table 5),
363 probably due to the damage of starch granules along with the degradation of amylopectin,
364 allowing more amylose to leach out and form stronger network and to co-crystallize with the
365 partially degraded amylopectin (with longer chain length than in WMS) more effectively.
366 Similar correlations were not observed from HAMS film with 40% plasticizer content, which
367 may be attributed to the lesser degree of damage to the starch granules (less shear energy)
368 than in those with 30% plasticizer content (Li, Hasjim, Xie, Halley & Gilbert, 2013).

369 Comparing all three types of starch films, an increase in amylose content increases the
370 elongation at break, which is consistent with previous studies (Li et al., 2011; Lourdin, Valle
371 & Colonna, 1995). The long branches of amylose (Liu, Halley & Gilbert, 2010; Vilaplana,
372 Hasjim & Gilbert, 2012) are more flexible than the short branches of amylopectin, and the
373 random coils of amylose branches can be easily stretched to give higher elongation at break;
374 however, the shorter branches of amylopectin molecules form a rigid (van Soest & Essers,
375 1997), inflexible network due to high molecular entanglements. The apparent correlation
376 between \bar{R}_h and the elongation at break was probably because starch with a higher amylose
377 content inherently has a smaller \bar{R}_h (Table 5).

378 As discussed above, the effective inter-molecular network formed by the longer chains of
379 amylose improves tensile mechanical properties of starch film (such as higher tensile
380 strength, Young's modulus), which is similar to the results from the studies of van Soest et al.
381 (van Soest, Benes & De Wit, 1995; van Soest, Benes, de Wit & Vliegenthart, 1996), where an
382 increase in starch molecular weight (longer branches with less acid hydrolysis) leads to a
383 higher tearing energy. Larger molecules normally have more molecular entanglements and
384 thus form a stronger network, which increases the energy required to tear the starch film
385 during tensile testing. As acid degrades starch molecules to a higher extent than the

386 degradation of starch molecules induced by extrusion, this phenomenon is not as apparent for
387 the films made from starch extrudates in the present study.

388 On the other hand, there were no significant correlations between starch structural
389 parameters (molecular size and amylose content) and the mechanical properties from the
390 different starches at 30% plasticizer content. At this level of plasticizer, the molecules might
391 be restrained in a more rigid network structure, preventing them from undergoing
392 retrogradation after extrusion and being fully stretched during tensile test. The results suggest
393 that plasticizer content is more dominant in governing the tensile mechanical properties of
394 starch film than amylose content and molecular size.

395 The degree of crystallinity of the starch films produced under different extrusion
396 conditions did not show significant correlations with tensile mechanical properties (Table 5).
397 In a previous paper (Li, Hasjim, Xie, Halley & Gilbert, 2013), it was noted that a proportion
398 of crystallinity in extruded samples was related to the starch granule remnants not completely
399 gelatinized during extrusion processing. The lack of a correlation between the starch
400 crystallinity prior to HTT and tensile mechanical properties implies that either the differences
401 in the degree of crystallinity were not large enough to induce changes in the tensile
402 mechanical properties, or this crystalline structure was originated from the starch granule
403 remnants and did not participate in the continuous network that influenced the tensile
404 mechanical properties. This is different from the inferences from the study by van Soest et al.
405 (van Soest, Hulleman, de Wit & Vliegenthart, 1996), which concluded that an increase in the
406 degree of crystallinity (by aging starch films at room temperature) led to an increase in elastic
407 modulus and tensile strength. This inconsistency brings the question of whether the
408 crystallinity source, i.e. within granular starch and that of the continuous network, has an
409 effect on the tensile mechanical properties. It should be noted that the ungelatinized starch

410 granules may act as "filler or defects" in the continuous structure, which may promote the
411 formation of microcracks, causing decreases in elongation at break (Bartczak, Argon, Cohen
412 & Weinberg, 1999); however, this was not observed to any extent in this study.

413 The higher degree of crystallinity of NMS film after HTT was accompanied by
414 significantly higher Young's modulus (Table 3). HTT was applied in the present study to
415 increase the crystallinity of the starch network surrounding the granular starch, allowing the
416 investigation of the effects of the crystalline structure from retrograded starch on the tensile
417 mechanical properties. It should be noted that only the crystalline structure was altered by
418 HTT, whereas molecular size (Chung, Hoover & Liu, 2009) and plasticizer content (Table 3)
419 were not changed. Thus the increased Young's modulus is due to the increased degree of
420 crystallinity after HTT, and greater entanglements may be formed in the continuous network
421 (melted molecules) of the starch films, which behaves like physical cross-linking, producing
422 greater resistance to chain mobility. Although there was some retrogradation in the starch
423 films aged at 54% RH for at least 14 days, the extent of rearranged crystallinity was less than
424 in those after HTT, which was carried out at a high-temperature, excessive-moisture
425 environment, providing greater chain mobility. This is confirmed by sharper crystalline peaks
426 in the XRD diffractograms (Figure 5) and higher melting temperature (Supporting
427 Information Table S1).

428 These results imply that the effects of crystallinity on starch mechanical properties are
429 more complicated than reported previously, such as by van Soest et al. (van Soest, Hulleman,
430 de Wit & Vliegthart, 1996). The crystalline structure originating from the starch granule
431 remnants did not affect the starch mechanical properties, but that of the starch network
432 surrounding the starch granule remnants controlled the starch mechanical properties. Thus, it
433 is important to understand the nature of the crystalline structure in starch film when

434 correlating with mechanical properties.

Accepted Manuscript

435

436 **5. Conclusion**

437 The effects of starch molecular, crystalline and granular structure on the mechanical
438 properties of starch films were examined. Degradation on the amylopectin molecules did not
439 cause any significant changes in mechanical properties, although the molecular size (\bar{R}_h)
440 range of the degraded waxy starch used here had a wide variation (38 – 58 nm). The shear
441 degradation of amylopectin induced by extrusion might be too small to show any significant
442 changes in the tensile mechanical properties. On the other hand, the longer branches of
443 amylose molecules played a more dominant role than \bar{R}_h in determining tensile mechanical
444 properties, as long amylose branches may form more inter- or intra-molecular flexible
445 network, increasing elongation at break. However, the effects of long branches on the
446 mechanical properties are limited when the plasticizer content is quite low. As distinct from a
447 previous finding, which did not separate the sources of crystallinity in TPS to explain their
448 roles in mechanical properties, the present study showed that the crystallization of leached-
449 out amylose in the continuous phase played a more dominant role on the mechanical
450 properties of TPS than the crystalline structure from the starch granule remnants, which is not
451 involved in the continuous network. The presence of native starch granules may act as defect
452 and negatively affect the mechanical properties (e.g. decrease in elongation). Thus in order to
453 obtain starch materials with superior mechanical properties, it is essential to increase the
454 crystallinity of the continuous phase and to use starches with longer branches, but lower
455 gelatinization temperature to maximize the amount of leached-out amylose. .

456 **Acknowledgement**

457 The authors acknowledge the facilities, and the scientific and technical assistance, of the
458 Australian Microscopy & Microanalysis Research Facility at the Centre for Microscopy and
459 Microanalysis, The University of Queensland, Brisbane, Australia. Financial assistance from
460 an Australian Research Council Discovery grant, DP130102461, is highly appreciated.

461 **Supporting information**

462 Supplementary data mentioned in the text is provided.

463 Figure S1. SEC weight distributions of extrudates from waxy and high-amylose maize
464 starches (WMS and HAMS, respectively) before and after compression molding (CM).

465 Figure S2: X-ray diffractograms of compress molded waxy and high-amylose maize starch
466 (WMS and HAMS, respectively) films before and after hydrothermal treatment (HTT).

467 Table S1. Thermal properties of normal maize starch films with and without hydrothermal
468 treatment.

469 Table S2: Tukey's pairwise comparison of mechanical properties of different starch films
470 from Table 1.^a

471

471

472 **References**

- 473 Cave, R. A., Seabrook, S. A., Gidley, M. J., & Gilbert, R. G. (2009). Characterization of
474 starch by size-exclusion chromatography: The limitations imposed by shear scission.
475 *Biomacromolecules*, *10*(8), 2245-2253.
- 476 Chen, P., Yu, L., Chen, L., & Li, X. (2006). Morphology and microstructure of maize
477 starches with different amylose/amylopectin content. *Starch - Stärke*, *58*(12), 611-615.
- 478 Chung, H.-J., Hoover, R., & Liu, Q. (2009). The impact of single and dual hydrothermal
479 modifications on the molecular structure and physicochemical properties of normal corn
480 starch. *International Journal of Biological Macromolecules*, *44*(2), 203-210.
- 481 Ferreira, F. A. B., Grossmann, M. V. E., Mali, S., Yamashita, F., & Cardoso, L. P. (2009).
482 Effect of relative humidities on microstructural, barrier and mechanical properties of Yam
483 starch-monoglyceride films. *Brazilian Archives of Biology and Technology*, *52*, 1505-1512.
- 484 Jane, J., Xu, A., Radosavljevic, M., & Seib, P. A. (1992). Location of amylose in normal
485 starch granules. I. Susceptibility of amylose and amylopectin to cross-linking reagents.
486 *Cereal Chemistry*, *69*, 405-409.
- 487 Li, M., Hasjim, J., Xie, F., Halley, P. J., & Gilbert, R. G. (2013). Shear degradation of
488 molecular, crystalline, and granular structures of starch during extrusion. *Starch - Stärke*, 1-
489 11.
- 490 Li, M., Liu, P., Zou, W., Yu, L., Xie, F., Pu, H., Liu, H., & Chen, L. (2011). Extrusion
491 processing and characterization of edible starch films with different amylose contents.
492 *Journal of Food Engineering*, *106*(1), 95-101.
- 493 Liu, H., Yu, L., Xie, F., & Chen, L. (2006). Gelatinization of cornstarch with different
494 amylose/amylopectin content. *Carbohydrate Polymers*, *65*(3), 357-363.
- 495 Liu, W.-C., Halley, P. J., & Gilbert, R. G. (2010). Mechanism of degradation of starch, a
496 highly branched polymer, during extrusion. *Macromolecules*, *43*(6), 2855-2864.
- 497 Lloyd, N. E., & Kirst, L. C. (1963). Some factors affecting the tensile strength of starch films.
498 *Cereal Chemistry*, *40*, 154-161.
- 499 Lopez-Rubio, A., Flanagan, B. M., Gilbert, E. P., & Gidley, M. J. (2008). A novel approach
500 for calculating starch crystallinity and its correlation with double helix content: A combined
501 XRD and NMR study. *Biopolymers*, *89*(9), 761-768.
- 502 Lourdin, D., Valle, G. D., & Colonna, P. (1995). Influence of amylose content on starch films
503 and foams. *Carbohydrate Polymers*, *27*(4), 261-270.
- 504 Mali, S., Sakanaka, L. S., Yamashita, F., & Grossmann, M. V. E. (2005). Water sorption and
505 mechanical properties of cassava starch films and their relation to plasticizing effect.
506 *Carbohydrate Polymers*, *60*(3), 283-289.

- 507 Mathew, A. P., & Dufresne, A. (2002). Plasticized waxy maize starch: effect of polyols and
508 relative humidity on material properties. *Biomacromolecules*, 3(5), 1101-1108.
- 509 Pérez, S., & Bertoft, E. (2010). The molecular structures of starch components and their
510 contribution to the architecture of starch granules: A comprehensive review. *Starch - Stärke*,
511 62(8), 389-420.
- 512 Shogren, R. L., & Jasberg, B. K. (1994). Aging properties of extruded high-amylose starch.
513 *Journal of environmental polymer degradation*, 2(2), 99-109.
- 514 Tabi, T., & Kovacs, J. G. (2007). Examination of injection moulded thermoplastic maize
515 starch. *Express Polymer Letters*, 1(12), 804-809.
- 516 Thunwall, M., Boldizar, A., & Rigdahl, M. (2006). Compression molding and tensile
517 properties of thermoplastic potato starch materials. *Biomacromolecules*, 7(3), 981-986.
- 518 Vamadevan, V., Bertoft, E., & Seetharaman, K. (2013). On the importance of organization of
519 glucan chains on thermal properties of starch. *Carbohydrate Polymers*, 92(2), 1653-1659.
- 520 van Soest, J. J. G., Benes, K., & De Wit, D. (1995). The Influence of acid hydrolysis of
521 potato starch on the stress-strain properties of thermoplastic starch. *Starch - Stärke*, 47(11),
522 429-434.
- 523 van Soest, J. J. G., Benes, K., de Wit, D., & Vliegthart, J. F. G. (1996). The influence of
524 starch molecular mass on the properties of extruded thermoplastic starch. *Polymer*, 37(16),
525 3543-3552.
- 526 van Soest, J. J. G., & Essers, P. (1997). Influence of amylose-amylopectin ratio on properties
527 of extruded starch plastic sheets. *Journal of Macromolecular Science, Part A* (Vol. 34, pp.
528 1665-1689): Taylor & Francis.
- 529 van Soest, J. J. G., Hulleman, S. H. D., de Wit, D., & Vliegthart, J. F. G. (1996). Changes
530 in the mechanical properties of thermoplastic potato starch in relation with changes in B-type
531 crystallinity. *Carbohydrate Polymers*, 29(3), 225-232.
- 532 Vilaplana, F., Hasjim, J., & Gilbert, R. G. (2012). Amylose content in starches: Toward
533 optimal definition and validating experimental methods. *Carbohydrate Polymers*, 88(1), 103-
534 111.
- 535 Walenta, E., Fink, H.-P., Weigel, P., & Ganster, J. (2001). Structure-property relationships in
536 extruded starch, 1 Supermolecular structure of pea amylose and extruded pea amylose.
537 *Macromolecular Materials and Engineering*, 286(8), 456-461.
- 538 Zhu, F., Bertoft, E., & Seetharaman, K. (2013). Characterization of internal structure of
539 maize starch without amylose and amylopectin separation. *Carbohydrate Polymers*, 97(2),
540 475-481.
- 541

541

542 **Figure captions**

543 Figure 2. SEM images of non-fractured (NF) and cryo-fractured (CF) surfaces of waxy
544 and high-amylose maize starch (WMS and HAMS, respectively) films before and after
545 compression molding (CM).

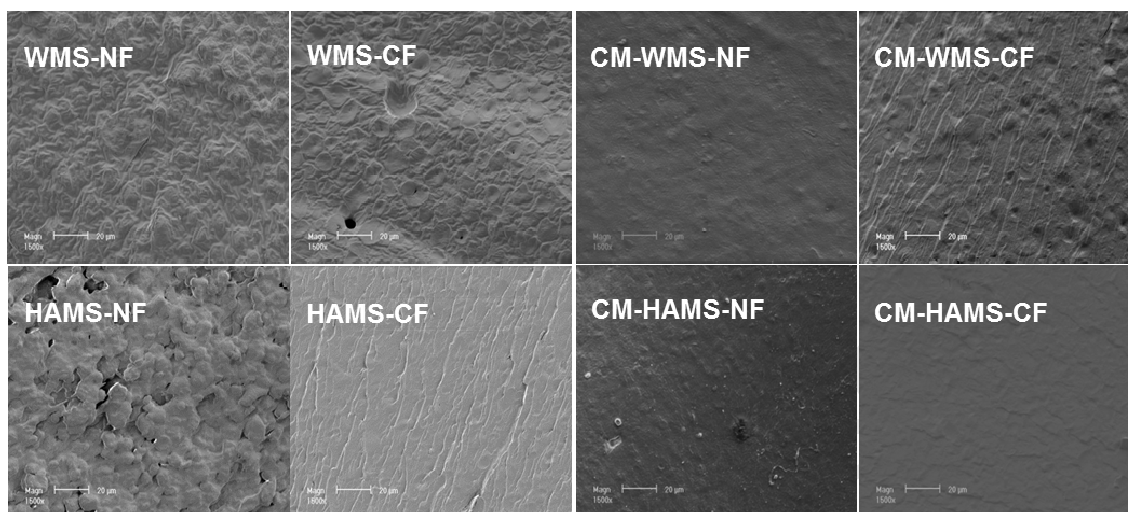
546 Figure 3. Moisture absorption curve of waxy (WMS, with filled symbols) and high-
547 amylose maize starches (HAMS, with open symbols) films stored at different relative
548 humidity (● for 33% RH, ■ for 54% RH, and ▲ for 75% RH)

549 Figure 4. X-ray diffractograms of compression molded starch films after being stored for
550 different times at 54% RH. Red arrows point at the peaks of V-type crystallinity. (A for waxy
551 maize starch films, B for normal maize starch films, and C for high-amylose maize starch
552 films)

553 Figure 5. X-ray diffractograms of compression molded normal maize starch extrudate
554 before and after hydrothermal treatment (HTT). The extrusion processing conditions of films
555 prior to compression molding are listed in Table 3.

556

556

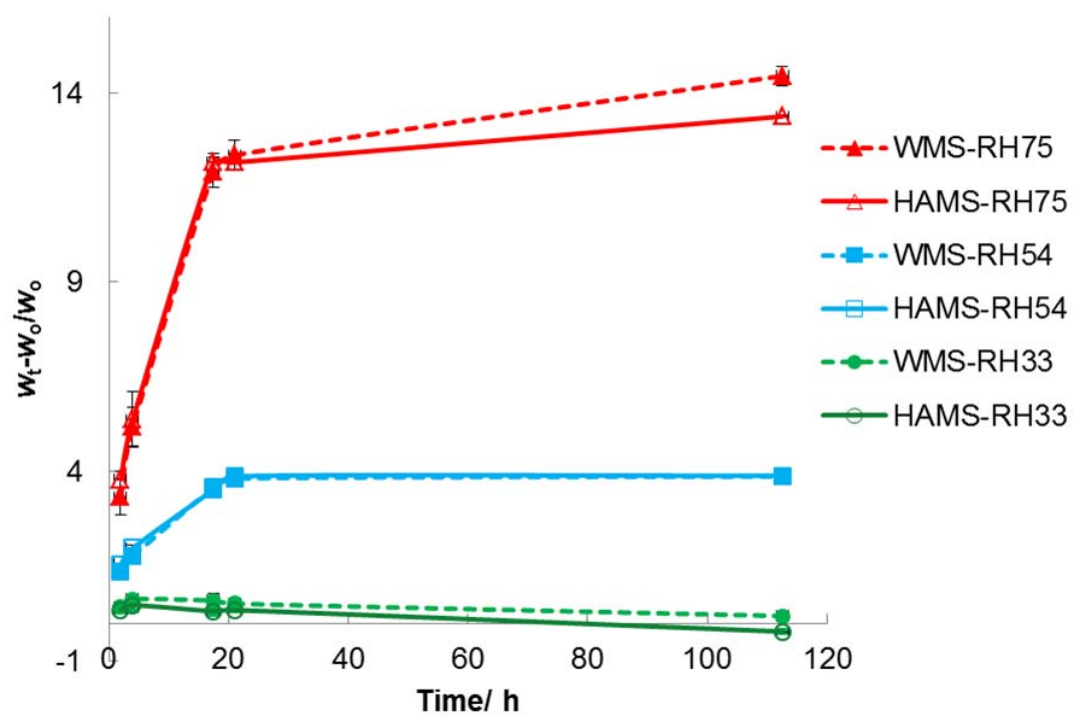


557

558 Figure 2

559

559

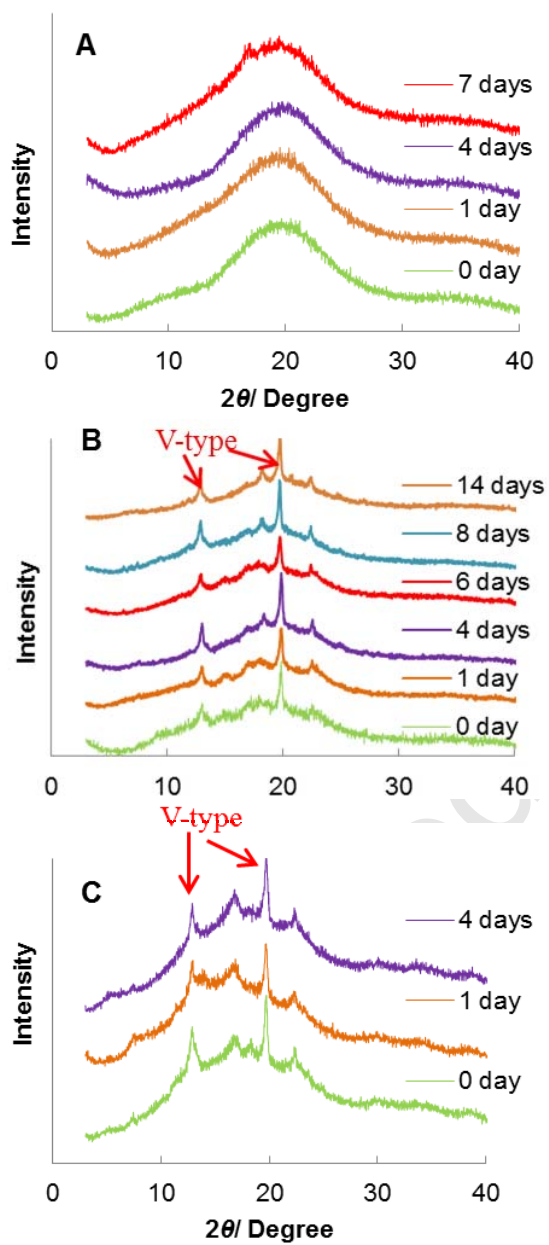


560

561 Figure 3

562

562

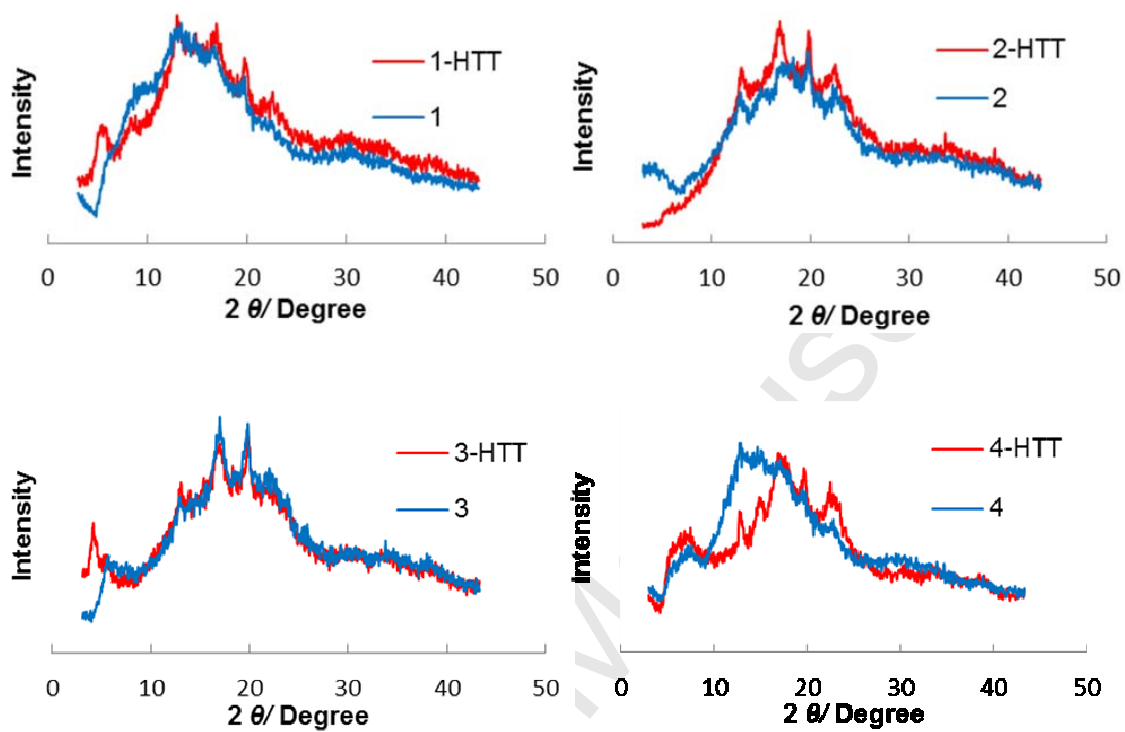


563

564 Figure 4

565

565



566

567 Figure 5

568 Table 1. Processing conditions, starch structure information of starch extrudates and the corresponding mechanical properties of the starch
 569 films ^a

Starch extrudate	Temperature °C	SS rpm	Plasticizer % ^b	\bar{R}_h / nm ^c	Crystallinity %	Tensile strength (MPa)	Young's Modulus (MPa)	Elongation at
WMS-1	105	70	40	85.7	22.2	9.4 ± 1.0 ^e CDE ^f	515 ± 56 B	6.2 ± 0.7 DE
WMS-2	105	130	40	88.8	20.2	8.3 ± 2.0 DE	365 ± 107 B	6.8 ± 2.0 DE
WMS-3	135	70	40	99.1	9.58	11.2 ± 0.4 BCDE	540 ± 71 B	6.2 ± 1.9 DE
WMS-4	135	130	40	96.7	11.2	10.2 ± 2.6 BCDE	542 ± 50 B	5.9 ± 3.9 DE
WMS-5	105	70	30	55.1	18.5	18.3 ± 2.1 BCDE	1401 ± 113 A	1.5 ± 0.6 E
WMS-6	105	130	30	38.4	9.03	14.8 ± 2.2 BCDE	1421 ± 49 A	1.6 ± 0.7 E
WMS-7	135	70	30	58.7	17.1	15.8 ± 2.8 BCDE	1453 ± 171 A	1.4 ± 0.2 E
WMS-8	135	130	30	41.4	17.7	19.1 ± 3.6 BCDE	1464 ± 261 A	1.7 ± 0.3 E
NMS-1	105	130	40	40.0	12.7	5.3 ± 0.5 E	217 ± 15 B	17.1 ± 2.1 BCD
NMS-2	135	70	40	48.0	11.4	8.2 ± 0.8 BCDE	388 ± 52 B	20.7 ± 1.7 AB
NMS-3	105	130	30	31.0	10.3	5.5 ± 0.3 E	332 ± 33 B	8.9 ± 1.4 CDE
NMS-4	135	130	30	30.0	13.9	8.4 ± 0.4 DE	613 ± 17 B	9.9 ± 1.0 BCDE
HAMS-1	105	70	40	9.3	9.48	11.6 ± 0.9 BCDE	645 ± 76 B	11.2 ± 2.2 BCDE
HAMS-2	105	130	40	10.1	9.18	12.7 ± 1.6 BCDE	676 ± 52 B	15 ± 2.4 BCD
HAMS-3	135	70	40	9.0	9.04	12.7 ± 1.1 BCDE	543 ± 95 B	18.9 ± 4.1 ABC
HAMS-4	135	130	40	9.4	9.99	14.5 ± 1.1 BCDE	623 ± 76 B	29 ± 4.0 A
HAMS-5	105	70	30	9.4	6.39	23.5 ± 3.6 ABC	1568 ± 85 A	2.2 ± 0.3 E
HAMS-6	105	130	30	9.9	7.36	22.0 ± 5.0 ABCD	1528 ± 73 A	2.1 ± 0.3 E
HAMS-7	135	70	30	9.3	8.72	24.5 ± 4.2 AB	1510 ± 141 A	2.5 ± 0.7 E
HAMS-8	135	130	30	8.5	9.33	35.0 ± 5.1 A	1898 ± 253 A	2.8 ± 0.6 E

570 ^a Extrudates are obtained in the previous study (Li, Hasjim, Xie, Halley & Gilbert, 2013)

571 ^b Plasticizer content is the amount of plasticizer used in extrusion, which is used to describe different films, whereas the aged films with same
572 plasticizer content may lose similar amount of moisture during storage

573 ^c \bar{R}_h , average hydrodynamic radius.

574 ^d The degree of crystallinity from compression molded starch materials after being stored at 54% relative humidity for 2 weeks

575 ^e Means \pm standard deviations

576 ^f Numbers in the same column with different letters are significantly different at $p < 0.05$

577

578 Table 2. Treatments and characterization methods for different thermoplastic starch
 579 extrudates.

Treatment	Extrudates ^a	Characterization
Untreated pellet	WMS-7 and HAMS-7	SEM, SEC
CM	WMS-7 and HAMS-7	SEM, SEC
CM and conditioning at 33, 54, and 75% RH	WMS-7, HAMS-7	Water absorption
CM and conditioning at 54% RH	All of WMS, NMS, and HAMS	Tensile test
CM, HTT, and conditioning at 54% RH	NMS-1, -2, -3, and -4	Tensile test, XRD, DSC

580 ^a The processing conditions of the extrudates are listed in Table 1

581

581

582 Table 3. Mechanical properties, degree of crystallinity, and moisture content of normal
 583 maize starch films before and after hydrothermal treatment ^a

Starch film ^b	Degree of crystallinity %	Moisture content ^c %	Tensile strength MPa	Young's Modulus MPa	Elongation at break %
NMS-1	11.2	12.7	5.3 ± 0.5 A ^d	217 ± 15 D	17.1 ± 2.1 A
NMS-1 HTT	13.0	11.3	8.6 ± 1.9 A	651 ± 107 AB	10.1 ± 1.3 AB
NMS-2	12.6	11.4	8.2 ± 0.8 A	388 ± 52 BCD	20.7 ± 1.7 A
NMS-2 HTT	22.2	11.0	10.2 ± 0.8 A	761 ± 50 A	9.9 ± 2.1 AB
NMS-3	15.3	10.3	5.5 ± 0.3 A	332 ± 33 CD	8.9 ± 1.4 AB
NMS-3 HTT	16.6	12.1	8.0 ± 1.1 A	784 ± 64 A	2.9 ± 1.2 B
NMS-4	13.2	13.9	8.4 ± 0.4 A	613 ± 17 ABC	12.9 ± 4.8 AB
NMS-4 HTT	24.2	11.0	10.2 ± 0.6 A	768 ± 48 A	7.8 ± 3.0 AB

584 ^a Numbers in the same column with different letters are significantly different at $p < 0.05$.

585 ^b The extrusion processing conditions of the film prior to compression molding are listed
 586 in Table 1

587 ^c Moisture content of film after being conditioning at 54% RH for 14 days

588 ^d Means ± standard deviations

589

589

590 Table 4. Mechanical properties of waxy and high-amylose maize starch films after being
591 stored at different relative humidities for 14 days.^a

Starch film ^b	Relative humidity (%)	Tensile strength (MPa)	Young's Modulus (MPa)	Elongation at break (%)
WMS-7	33	13.6 ± 2.8 BC ^c	1940 ± 171 A	0.9 ± 0.2 A
WMS-7	54	15.8 ± 2.8 BC	1453 ± 171 A	1.4 ± 0.2 A
WMS-7	75	5.2 ± 1.1 C	197 ± 42 B	10.1 ± 3.0 A
HAMS-7	33	34.8 ± 4.5 A	1944 ± 223 A	4.2 ± 1.0 A
HAMS-7	54	24.5 ± 4.2 AB	1510 ± 141 A	2.5 ± 0.7 A
HAMS-7	75	8.7 ± 1.2 BC	256 ± 70 B	23.1 ± 2.7 B

592 ^a Numbers in the same column with different letters are significantly different at $p < 0.05$.

593 ^b The extrusion processing conditions of the film prior to compression molding are listed
594 in Table 1

595 ^c Means ± standard deviations

596

597

597

598 Table 5. Correlations between starch structures and the tensile mechanical properties of
 599 starch films stored at 54% RH ^a

Samples	Tensile mechanical properties	Amylose content	\bar{R}_h	Crystallinity
WMS films with 40% plasticizer content	Elongation at break	NA	-0.487	0.561
	Tensile strength	NA	0.820	-0.845
	Young's modulus	NA	0.492	-0.556
WMS films with 30% plasticizer content	Elongation at break	NA	-0.886	-0.225
	Tensile strength	NA	0.060	0.776
	Young's modulus	NA	-0.467	0.320
HAMS films with 40% plasticizer content	Elongation at break	NA	-0.176	0.645
	Tensile strength	NA	0.045	0.632
	Young's modulus	NA	0.876	0.232
HAMS films with 30% plasticizer content	Elongation at break	NA	-0.946	0.888
	Tensile strength	NA	-0.954* ^b	0.743
	Young's modulus	NA	-0.895	0.458
All the three types of films with 40% plasticizer content	Elongation at break	0.749*	-0.756*	-0.456
	Tensile strength	0.517	-0.454	-0.483
	Young's modulus	0.377	-0.314	-0.350
All the three types of films with 30% plasticizer content	Elongation at break	0.158	-0.090	-0.048
	Tensile strength	0.492	-0.526	-0.307
	Young's modulus	0.140	-0.206	-0.121
				Δ Crystallinity
NMS films before and after HTT	Δ Elongation at break			0.409
	Δ Tensile strength			0.978*
	Δ Young's modulus			0.413

600 ^a WMS, NMS, and HAMS represent for waxy maize starch, normal maize starch and high
 601 amylose starch.

602 ^b Significant correlations ($p < 0.05$) are represented by *, very significant correlations
 603 ($p < 0.01$) are represented by **. The numbers in the table are the correlation coefficients.

604 $^{\circ}\Delta$ crystallinity is the different values between the degree of crystallinity before and after

605 HTT (values are shown in Table 3)

606

Accepted Manuscript

606

607 Highlights:

608

609 - Thermoplastic starches (TPS) are “green” but mechanical properties are often poor

610 - The properties of TPSs were related with varied molecular and crystalline structures
611 induced by extrusion

612 - Crystalline structure had the greatest effect

613 - Mechanisms of property enhancement were explored

614 - Amylopectin degradation induced by extrusion did not affect mechanical properties

615

616

Accepted Manuscript